

Subscriber access provided by NANJING UNIV

**Article** 

# **Computer Simulations of Vesicle Fission Induced by External Amphipathic Inclusions**

Kai Yang, and Yu-qiang Ma

J. Phys. Chem. B, 2009, 113 (4), 1048-1057 • DOI: 10.1021/jp805551s • Publication Date (Web): 06 January 2009

Downloaded from http://pubs.acs.org on February 4, 2009

# **More About This Article**

Additional resources and features associated with this article are available within the HTML version:

- Supporting Information
- Access to high resolution figures
- Links to articles and content related to this article
- Copyright permission to reproduce figures and/or text from this article

View the Full Text HTML



# Computer Simulations of Vesicle Fission Induced by External Amphipathic Inclusions

# Kai Yang and Yu-qiang Ma\*

National Laboratory of Solid State Microstructures, Nanjing University, Nanjing 210093, China Received: June 24, 2008; Revised Manuscript Received: November 05, 2008

Fission is an important biological phenomenon to maintain normal functions of cells, but its mechanism is not quite clear. In this paper, the fission behaviors of a two-component lipid vesicle induced by external amphipathic inclusions are studied by the dissipative particle dynamics method. We find that the fission of the lipid domain the in a spherical vesicle will occur only when the concentration of amphipathic inclusions is beyond a threshold concentration. It reveals that this kind of fission is induced by the combination of the domain's line tension and the asymmetric distribution of the amphipathic inclusions in the membrane's inner and outer leaflets. Furthermore, we also find that the fission behaviors are influenced by the area-to-volume ratio of vesicles and the structure characters of amphipathic inclusions (e.g., chain length and rigidity). Especially, the chain length and rigidity of amphipathic inclusions have complicated effects on the vesicle fission. With the variation of these factors, the fission process will be accelerated or delayed. The present study is helpful to understand the possible fission mechanism of lipid bilayers with embedded proteins.

### I. Introduction

Fission is a vital biological process of cellular membranes. It is ubiquitous in cells, such as cell division, membrane budding from the Golgi apparatus and endoplasmic reticulum, endocytosis, exocytosis, and so forth. Fission is always accompanied by the shape transformation of cellular membranes. However, because of the complexity of the cellular membrane, the mechanism of the fission and the manner of shape transformation of membranes are still largely elusive.

In cellular membranes, there is a variety of proteins and lipids, and the structures and functions of most of these proteins and lipids are not very clear yet. It is generally accepted that the basic structure of the membrane is a lipid bilayer, in which the polar head of lipids is oriented toward an aqueous environment to screen the hydrophobic acyl chains of lipid molecules. Different kinds of lipids distribute heterogeneously in the membrane and organize into complexes or domains, so-called lipid rafts.<sup>2,3</sup> Such a phase-segregated behavior has been observed experimentally in model membranes, for example, the sphingolipids with saturated acyl tail chains can form the liquidordered (l<sub>o</sub>) domains with cholesterol, whereas the phospholipids with unsaturated acyl chains can form liquid-disordered (l<sub>d</sub>) domains. 4,5 The minimization of the line tension between different lipid domains could drive the shape deformation of the membranes or the fission of domains in multicomponent lipid bilayers under appropriate conditions. In experiments, typical shape deformations of the membrane and fission behaviors have been observed in lipid giant unilamellar vesicles (GUVs) or liposomes.<sup>6-8</sup>

However, it is generally believed that most of the fission behaviors in living cells occur with the aid of proteins. Much attention has now been paid to two classes of proteins which regulate the curvature of the membrane in different fashions. It has been discovered in some experiments that protein epsin can.transform the liposomes into small tubules. In the epsin family, the most conserved structure is the globular amphipathic

ENTH (epsin N-terminal homology) domain. Ford et al. 9 found that the mutation of the hydrophobic region of the ENTH helix prevents the shape transformation of liposomes. They speculate that the insertion of the ENTH domain into the lipid bilayer results in the curvature of the membrane. Additionally, another class of proteins, such as amphiphysin, nadrins, olugophrenins, and sorting nexins, is also relevant with the cell fission. This class of proteins owns a similar region, the BAR domain ("Bin, amphiphysin, Rvs" domain). 10-13 The BAR domain is a dimer of two kinked monomers which forms a rigid banana-shaped structure. As a scaffold, the BAR domain could bind its concave region to the membrane and bend it. However, it has been found that there is an amino terminal amphipathic  $\boldsymbol{\alpha}$  helix in the BAR domain of some proteins. This amphipathic region is proposed to insert into the membrane to enhance the liposome tubulation as the protein epsin does. 11,13 On the basis of these experiments, one could find that, despite the diversity of the structure of proteins, the amphipathic structure and its insertion into the lipid bilayer indeed play special roles in shape deformation of the membrane. In recent experiments, Yamazaki and co-workers 14,15 observed the fission phenomena of GUVs of the lo-phase membrane induced by a series of the long-chain amphiphiles. They think that the allocation of amphiphiles into the external monolayer of the l<sub>0</sub> domain from the aqueous environment drives the shape deformation and fission of GUVs. They also found that the concentration of amphiphiles is crucial to the occurrence of vesicle fission. Actually, fission is an extremely complex process involved with different kinds of proteins and lipids, and there exists still a lot of unsolved issues. For example, what is the influence of the depth of the insertion and the orientation of the embedded inclusions?<sup>16</sup> What is the influence of the molecular structure of inclusions on the fission? Fission always occurs within several nanometers in size and is shorter than microseconds in time. Therefore, even for the simplest model of GUVs with the embedded inclusions, it is very difficult for experiments to entirely unveil the fission mechanism now. On the other hand, most current theoretical studies only concentrate on the pure lipid-mediated fission, and the fission models induced by external inclusions are scarce. Thus, more theoretical

<sup>\*</sup> To whom correspondence should be addressed. E-mail: myqiang@nju.edu.cn.

**Figure 1.** Coarse-grained model of (a) lipid A, (b) lipid B, (c) the amphipathic inclusion, and (d) water (blue: head beads of lipid A; light blue: tail beads of lipid A; yellow: head beads of lipid B; light green: tail beads of lipid B; red: hydrophilic head beads of inclusion; green: hydrophobic tail beads of inclusion; gray: water).

and computational simulation works are needed to systematically understand the effect of the structure characters and the fashion of insertion of amphipathic inclusions on the vesicle fission. Furthermore, these studies may have possible potential applications in biotechnology such as pharmaceutical preparation, cosmetics, and so forth.

Budding and fission in multicomponent lipid bilayers are theoretically studied with the continuum model, <sup>17,18</sup> whereas the molecular detail of lipids is ignored. To examine the dynamics of budding and fission, computer simulation becomes a powerful tool. Molecular dynamics (MD) simulations have offered us more insights into the cellular membranes. 19,20 Nevertheless, the small system size and time scale are restricted in MD simulations. To overcome these problems, coarse-gained (CG) simulation methods have been employed.<sup>21-23</sup> Dissipative particle dynamics (DPD) is an effective coarse-gained simulation method and has been extensively employed in soft matter systems. DPD is a mesoscopic simulation technique with hydrodynamic interaction, where each DPD particle is composed of a group of atoms or molecules. The soft interaction between DPD particles allows a larger simulation time step and space scale. Recent studies have shown that DPD simulation could reproduce proper characters of lipid bilayers, such as density distribution and surface stress profile, and mimic some important dynamics behaviors of the membrane.<sup>24–28</sup>

In this paper, we apply DPD method to study the behaviors of the budding and fission of a two-component lipid vesicle induced by external amphipathic inclusions. We use a simple bead-spring-based model to mimic the external amphipathic inclusions and obtain a detailed fission process of the lipid domain of the vesicle. The effects of the concentration, chain length, and rigidity of amphipathic inclusions are examined, and the possible mechanisms related to shape transformation and fission induced by amphipathic inclusions are discussed. We find that the vesicle fission process could be accelerated, delayed, or even be prevented by these factors. In addition, we also investigate the effect of the area-to-volume ratio of the vesicle on the fission behaviors.

The structure of the present paper is as follows: In section II, the DPD simulation model and technique are presented. In section III, the results of the simulation are described. Finally, the Discussion and Conclusion are given in sections IV and V, respectively.

### II. Model and Simulation Method

# **A. DPD Model of the Lipid and Amphipathic Inclusion.** In our simulations, the lipid molecule is modeled as a linear chain with two hydrophilic head beads (H) and five hydrophobic tail beads (T). These beads are connected by the harmonic springs. There are two kinds of lipids (A and B; see Figure 1a and b). The introduction of lipid B is to form a domain in the

matrix of lipids A; therefore, two kinds of lipids are chosen to

segregate from each other. For the sake of simplification, the architecture of the amphipathic inclusion is modeled similarly to that of lipids, namely, it consists of two hydrophilic head beads ( $H_p$ ) and several hydrophobic tail beads ( $T_p$ ) (Figure 1c). In order to investigate the influence of the structure of inclusions, the chain rigidity and tail bead number ( $n_T$ ) of amphipathic inclusions could vary in the simulations. Additionally, water is explicitly included in the system as the solvent.

**B. DPD Simulation Method.** DPD was first introduced by Hoogerbrugge and Koelman<sup>29</sup> to describe the mesoscopic hydrodynamic behaviors of complex fluids and later improved by Espagnol and Warren.<sup>30</sup> The evolution of the position and velocity of DPD bead i, ( $\mathbf{r}_i$ ,  $\mathbf{v}_i$ ), obeys Newton's equation of motion. In the DPD, there are three types of pairwise forces acting on bead i by bead j, the conservative force  $\mathbf{F}_{ij}^{\mathbf{C}}$ , dissipative force  $\mathbf{F}_{ij}^{\mathbf{C}}$ , and random force  $\mathbf{F}_{ij}^{\mathbf{R}}$ .

The conservative force  $\mathbf{F}_{ij}^{\mathbf{C}}$  is taken as

$$\mathbf{F}_{ij}^{\mathbf{C}} = \begin{cases} a_{ij} \left( 1 - \frac{r_{ij}}{r_{c}} \right) \hat{\mathbf{e}}_{ij} & r_{ij} < r_{c} \\ 0 & r_{ij} \ge r_{c} \end{cases}$$
 (1)

where  $\mathbf{r}_{ij} = \mathbf{r}_i - \mathbf{r}_j$ ,  $r_{ij} = |\mathbf{r}_{ij}|$ , and  $\hat{\mathbf{e}}_{ij} = \mathbf{r}_{ij}/r_{ij}$ . The parameter  $r_{\rm c}$  is the cutoff radius of the conservative force, and  $a_{ij}$  represents the maximum repulsion interaction of beads of type i and type j.

The dissipative force  $\mathbf{F}_{ij}^{D}$  is

$$\mathbf{F}_{ij}^{\mathrm{D}} = \begin{cases} -\gamma \left(1 - \frac{r_{ij}}{r_{\mathrm{c}}}\right)^{2} (\hat{\mathbf{e}}_{ij} \cdot \mathbf{v}_{ij}) \hat{\mathbf{e}}_{ij} & r_{ij} < r_{\mathrm{c}} \\ 0 & r_{ij} \ge r_{\mathrm{c}} \end{cases}$$
(2)

where  $\mathbf{v}_{ij} = \mathbf{v}_i - \mathbf{v}_j$  is relative velocity between beads i and j and  $\gamma$  is the strength of friction.

Finally, the random force  $\mathbf{F}_{ii}^{R}$  takes the form of

$$\mathbf{F}_{ij}^{R} = \begin{cases} \sqrt{2\gamma k_{\mathrm{B}}T} \left(1 - \frac{r_{ij}}{r_{\mathrm{c}}}\right) \zeta_{ij} \Delta t^{-1/2} \hat{\mathbf{e}}_{ij} & r_{ij} < r_{\mathrm{c}} \\ 0 & r_{ij} \ge r_{\mathrm{c}} \end{cases}$$
(3)

Here,  $\zeta_{ij}$  is a symmetric random variable with zero mean and unit variance, that is,  $\langle \zeta_{ij}(t) \rangle = 0$  and  $\langle \zeta_{ij}(t) \zeta_{i'j'}(t') \rangle = (\delta_{ii'}\delta_{jj'} + \delta_{ii'}\delta_{ii'})\delta(t-t')$ . The  $\Delta t$  is the time step of simulation.

In order to ensure the integrality of lipids and amphipathic inclusions, the harmonic spring interaction is applied between neighboring beads in a single molecule as follows

$$\mathbf{F}_{s} = -k_{s} \left( 1 - \frac{r_{i,i+1}}{l_{0}} \right) \hat{\mathbf{e}}_{i,i+1}$$
 (4)

where  $l_0$  is the equilibrium bond length and  $k_{\rm s}$  is the spring constant. The rigidity of lipid tails and amphipathic inclusions is denoted by a three-body bond angle potential  $U_{\rm a}^{24}$ 

$$U_a = k_a (1 - \cos(\varphi - \varphi_0)) \tag{5}$$

where  $\varphi$  is the bond angle of the two bonds connecting three beads i-1, i, and i+1 and  $\varphi_0$  is the preferred angle.

TABLE 1: Interaction Parameters of Bead–Bead Pairs,  $a_{ii}$ 

$a_{ij}$	W	$H_{A}$	$T_{A}$	$H_{B}$	$T_{B}$	$H_p$	$T_p$
W	25	25	95	25	95	25	120
$H_A$	25	25	95	40	95	40	95
$T_A$	95	95	25	95	40	95	40
$H_{B}$	25	40	95	25	95	25	95
$T_{B}$	95	95	40	95	25	95	25
$H_p$	25	40	95	25	95	25	95
$T_{p}$	120	95	40	95	25	95	25

TABLE 2: Some Simulation Parameters of Lipids and Inclusions

	$k_{\rm s}$	$l_0$	$k_{\rm a}$	$arphi_0$
lipid A	128	0.5	5	0
lipid B	128	0.5	5	0
inclusion	128	0.5	$k_b$	0

Our simulations apply the DPD Velocity-Verlet integration algorithm<sup>31</sup> and the integration time step  $\Delta t = 0.05$ . In addition, we choose the cutoff radius  $r_c$ , bead mass m, and temperature  $k_B T$  as the simulation units.

**C.** Simulation Parameters and Initial Configuration. All simulations are performed in the NVT ensembles at the temperature  $k_{\rm B}T=1$ . The size of the simulation box is 42 × 42 × 42 with the number density of  $\rho=3$ . There are a total of 222 264 DPD beads in the simulation box, and the periodic bound conditions are adopted in three directions.

The detailed value of the repulsion interaction  $a_{ij}$  and other simulation parameters are summarized in Tables 1 and 2. Especially, for the lipids, we set  $a_{H_A,H_B} = 40$  and  $a_{T_A,T_B} = 40$  to realize the phase separation of lipids A and B. The bond angle potential parameter  $k_a = 5$  for lipids is selected to well produce the phase behaviors of lipid molecules and mechanical character of lipid bilayers.<sup>28</sup> For the amphipathic inclusions, to ensure that the hydrophobic tails of the inclusions are sufficiently shielded from the aqueous environment, we set a larger value between their tail beads and water as  $a_{\rm WT_p} = 120$ . Since it has been found in experiments<sup>14,15</sup> that vesicle fission induced by amphiphiles could occur only when amphiphiles are located in the l<sub>o</sub> domain, we assume that the inclusions have a good affinity with the lipids B, and the values of  $a_{ij}$  are taken as  $a_{H_DH_B} = 25$ ,  $a_{\rm H_pH_A} = 40$  and  $a_{\rm T_pT_B} = 25$ ,  $a_{\rm T_pT_A} = 40$ . The bond angle potential parameter of the amphipathic inclusions  $k_b$  can vary between 0 and 30.

The vesicle used in our simulations is prepared by randomly distributing 3200 A-type lipids in the inner and outer leaflets of a nearly closed spherical surface.<sup>26</sup> In order to ensure that the vesicle is near zero surface tension, two holes are opened at the top and bottom of the vesicle at the beginning, respectively. Then 50 000 iterations are carried out to close the two holes and equilibrate the system. After equilibrium, the vesicle is closed and nearly spherical (Figure 2), and there are about 7418 water beads inside of the vesicle. Vesicles with different area-to-volume ratios can be realized by removing some water beads from its interior to the exterior region. Here, the area-to-volume ratio,  $\Pi$ , is defined as the ratio of the number of lipid beads to the total beads inside of the vesicle. With the increase of the area-to-volume ratio, the excess area of the vesicle will also increase. 32,33 In order to form the domain, some lipids A at the top of the vesicle are replaced by lipids B. Amphipathic inclusions are then introduced by a random distribution in a spherical shell whose thickness is  $1r_c$  (Figure 2). The center of the shell is located at the center of the vesicle, but its inner radius is  $0.25r_c$  longer than the outer radius of the

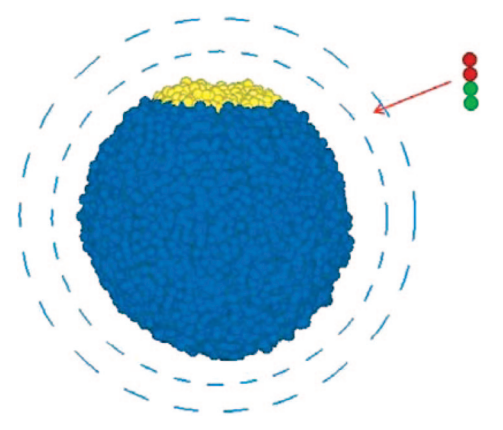


**Figure 2.** Initial configuration of the vesicle, domain, and inclusions. Lipid A is represented by blue color, and lipid B is yellow. The dashed circle shell represents the initial location of the inclusions.

vesicle. In experiments, the adding of inclusions near a vesicle can be achieved by a micropipet.<sup>14</sup> To save computer time, we put inclusions close to the vesicle. Because of their hydrophobic tails, inclusions will spontaneously enter the membrane of the vesicle to decrease the Gibbs free energy.

### **III. Simulation Results**

# A. Effect of the Concentration of Amphipathic Inclusions.

After vesicle formation composed of pure lipids A, 6% of lipid A is replaced by lipid B, and a single domain composed of lipid B is then formed on the vesicle. Figure 3a shows a snapshot of the vesicle with the lipid B domain in the absence of inclusions after long enough simulation iterations. Although the shape of the vesicle is slightly deformed, the domain does not bud or fission. Usually, there exists a line tension on the boundary of the domain due to the incompatibility of two kinds of lipids. However, because the repulsive interactions between lipids A and B are relatively weak, no budding or fission will occur in the vesicle that we studied, even when area-to-volume ratio  $\Pi$  are further increased from 0.81 to 0.84.

Now, we add some external amphipathic inclusions into the simulation box. Interestingly, when the number of the inclusions is high enough, the fission of the domain in the spherical vesicle occurs. The completely separated configuration of the lipids B domain and the vesicle with 320 external amphipathic inclusions is presented in Figure 3b and c. The domain of lipid B finally forms a new daughter vesicle. Additionally, an inspection of the cross section of the daughter vesicle (Figure 3c) clearly shows that the tails of amphipathic inclusions are embedded into the interior of the lipid bilayer. By comparing the vesicle configurations before and after the introduction of inclusions, we can conclude that this kind of vesicle fission is induced mainly by the insertion of external amphipathic inclusions into the lipid bilayer.

The detailed fission process of domain is presented in Figure 4. First, most of inclusions surround the vesicle. The vesicle begins to deform, and the domain of lipid B protrudes outward (Figure 4a,a'). Subsequently, the inclusions are embedded into the vesicle, and more inclusions tend to assemble in the domain. Meanwhile, a bud is formed obviously (Figure 4b,b'). As the system elapses in time, the domain deforms into a tubular shape (Figure 4c,c'). Then, the bud further bends, its neck becomes narrow, and the rim of the domain begin to fuse (Figure 4d,d'). Finally, a small vesicle composed of lipid B and amphipathic inclusions is separated from the parent vesicle (Figure 4e,4e').

However, fission does not occur in all cases of the existence of the amphipathic inclusions. We find that the concentration

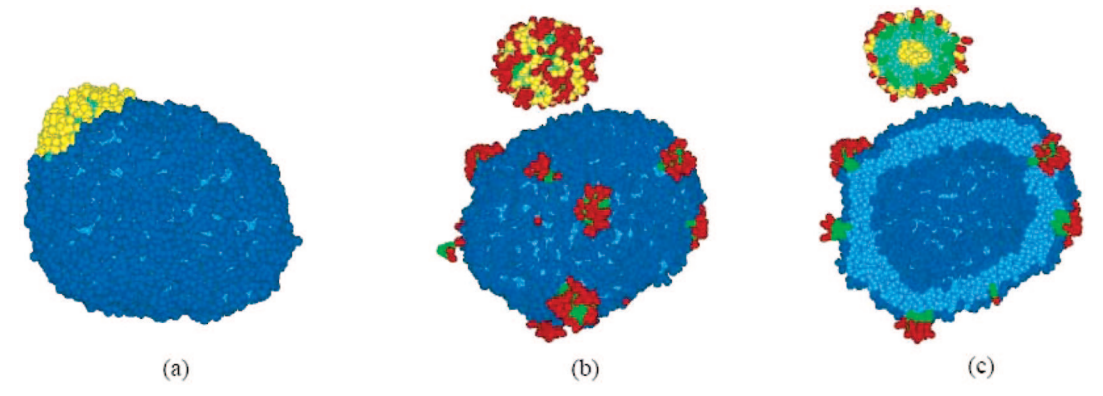


Figure 3. Final snapshots of the vesicle and domain without (a) and with (b) external amphipathic inclusions. (c) Cross-sectional image of (b). For (b) and (c), there are 320 amphipathic inclusions.  $n_T = 2$ ,  $k_b = 30$ , and  $\Pi = 0.81$ . Water beads are not displayed.

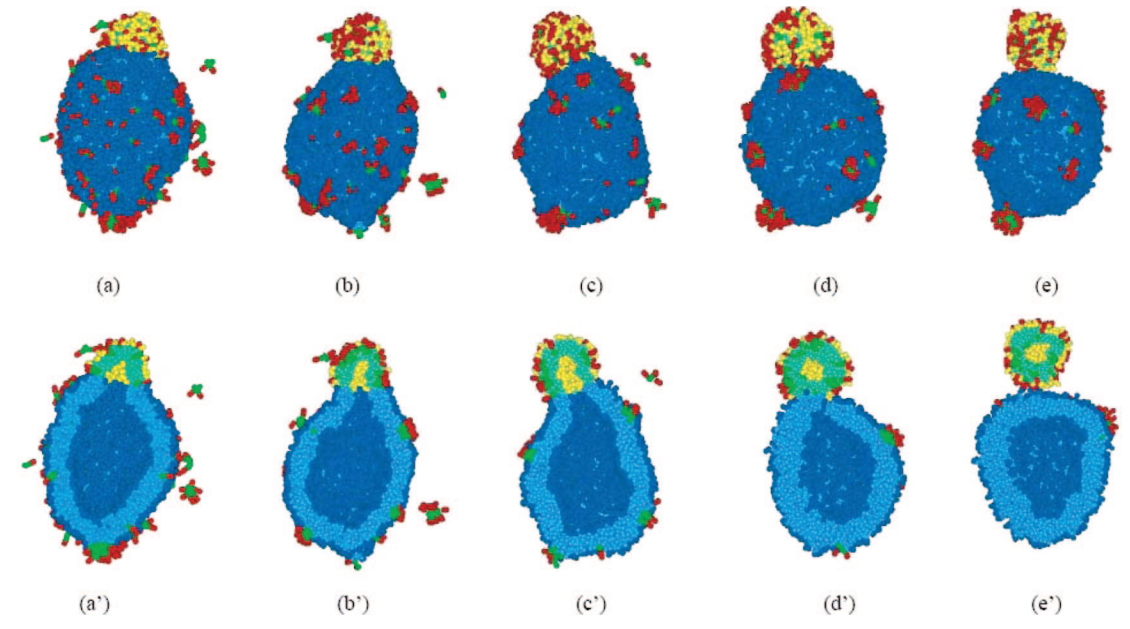


Figure 4. Fission process of the vesicle induced by the external amphipathic inclusions. The images are taken at (a) 6000, (b) 20 000, (c) 86 000, (d) 106 000, and (e) 118 000 simulation steps. Correspondingly, (a'-e') are their cross-sectional images.  $n_T = 2$ ,  $k_b = 30$ , and  $\Pi = 0.81$ .

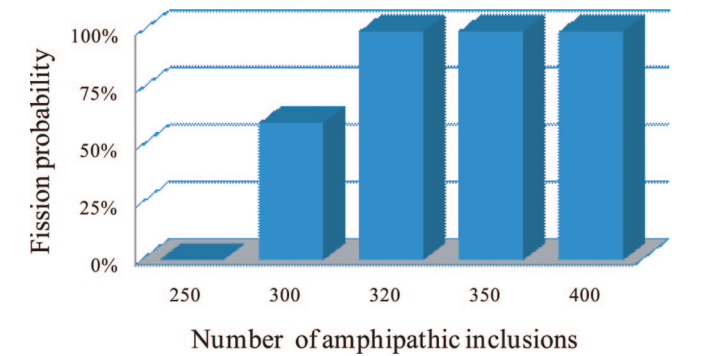
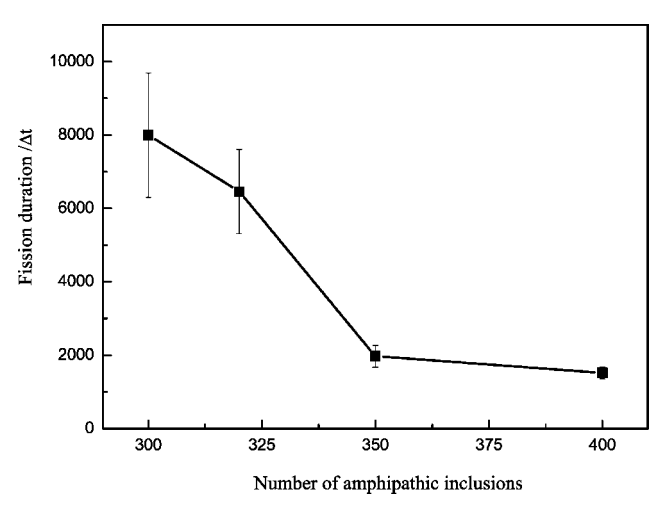


Figure 5. Fission probability of the vesicle with different numbers of inclusions.  $n_T = 2$ ,  $k_b = 30$ , and  $\Pi = 0.81$ .

of inclusions plays a key role in the fission processes. Figure 5 shows the fission probability of the domain of lipid B with different numbers of amphipathic inclusions. To examine such a fission probability, at least five independent simulation runs are conducted in each case with a fixed concentration of inclusions. As shown in Figure 5, there exists a threshold number of amphipathic inclusions for the occurrence of vesicle fission (here, the threshold number of inclusions is 300), and fission can be observed only when the number of inclusions is beyond this threshold value. Similar experimental phenomena have been observed by Yamazaki and co-workers, 14,15 while a direct comparison is difficult due to the huge size difference between our vesicle and the GUVs. However, it should be helpful to give insight into such interrelated fission behaviors. Furthermore, some differences still exist in different fission processes when the number of inclusions is beyond the threshold number. Figure 6 shows the fission duration of the domain with different numbers of amphipathic inclusions (when the number of inclusions is 300, we only include the cases in which the fission occurs). Here, the fission duration is defined as the period from the beginning of the simulation to the time when the interface length of the domain becomes zero. It is shown from Figure 6 that the fission duration decreases rapidly with the increase of the inclusion content. The interval of the longest and the shortest duration of fission is about  $6500\tau$ .

The other factors such as domain size, lipid chain rigidity, and line tension will also influence vesicle fission behaviors induced by external amphipathic inclusions. Some threshold numbers of amphipathic inclusions for the occurrence of vesicle fission under different conditions are summarized in Table 3. In the first six simulations (S-1-S-6), line tensions vary from 30 to 50. When the line tension is sufficiently strong (S-1 and S-2,  $a_{H_A,H_B} = 50$ ,  $a_{T_A,T_B} = 50$ ), fission can occur without any external inclusions. In this case, vesicle fission is completely



**Figure 6.** Fission duration of the vesicle with different numbers of amphipathic inclusions.  $n_T = 2$ ,  $k_b = 30$ , and  $\Pi = 0.81$ .

TABLE 3: Some Threshold Numbers of Amphipathic Inclusions for Vesicle Fission with Different Domain Size, Line Tension  $(a_{\rm H_A,H_B}, a_{\rm T_A,T_B})$  and Lipid Chain Rigidity  $(k_a)$   $(n_{\rm T}=2, k_{\rm b}=30, {\rm and}~\Pi=0.81)$ 

, ,	,		<i>'</i>	
SN	domain size	$k_{\rm a}$	line tension	threshold number
S-1	6%	5	50	0
S-2	12%	5	50	0
S-3	6%	5	40	300
S-4	12%	5	40	320
S-5	6%	5	30	∞
S-6	12%	5	30	∞
S-7	6%	30	40	400
S-8	6%	50	40	∞

caused by the phase separation of the domain from the vesicle with sufficient excess area. However, if line tension is small (S-5 and S-6,  $a_{H_A,H_B} = 30$ ,  $a_{T_A,T_B} = 30$ ), the domain only bulges outward to form a bud, but it cannot undergo fission for the vesicles whose size we studied, no matter how many external inclusions are inserted. Therefore, phase separation plays an essential role for the inclusions-induced vesicle fission. Furthermore, phase separation produces the boundary of the domain which can restrict the lateral movement of the B-type lipids within the domain. Thus, the strain caused by the insertion of the external inclusions will not be easily released. This can result in the deformation of the domain. For example, if the vesicle is just composed of one kind of lipid (lipid A or B), even with the existence of enough external inclusions, the vesicle is only deformed into prolate or elliptical shape, and no fission will occur (data not shown). For simulations S-3 and S-4, the only difference between their simulation conditions is the domain size. For the bigger domain, more external inclusions are required for the vesicle fission. In addition, the rigidity of lipid tails will evidently change the value of the threshold number (S-3, S-7, and S-8). With the increase of the chain rigidity, the lipid bilayer becomes "hard", the bending modulus increases, and thus, the threshold number also increases. In S-7,  $k_a$ increases to 30; the threshold number also increases to 400. For  $k_a = 50$ , the bilayer becomes rather hard, and no fission can occur (S-8).

In addition, because of the complicated fission process, there still exist some factors that influence its occurrence. For example, the high curvature of a rather small vesicle or liposome is possible to prevent the occurrence of the vesicle fission, and the small domain size may also suppress the occurrence of the fission. In order to examine these influences

on our simulation results, we have carried out additional simulations using a larger vesicle composed of 6400 lipids, where three domain sizes of 3, 6, and 10% are investigated. Furthermore, to exclude the possible artifact due to the large integration time step, 35 a small integration time step of  $\Delta t =$ 0.01 is applied. For all cases, the similar fission behaviors as those mentioned above are observed. The two-component vesicle could not undergo fission unless enough external inclusions (e.g., 400 inclusions) were introduced when the area-to-volume ratio was 0.71 or even 0.745. Therefore, neither the decrease of the curvature of parent vesicle nor the increase of the domain size and excess area could cause vesicle fission. This means that fission behaviors observed in our simulations are not caused by the phase separation of the lipid domain from the vesicle with sufficient excess area. On the other hand, the relatively small size of the domain and vesicle used in our simulations will perhaps slow the fission process, but it does not suppress the occurrence of the domain fission. In order to save simulation time, we still adopt the vesicle composed of 3200 lipids in the following study.

B. Effect of the Structure of Amphipathic Inclusions: Tail **Length and Chain Rigidity.** The amphipathicity of inclusions will result in the insertion of their hydrophobic tail into the lipid bilayer, and thus, the length and rigidity of inclusions can change their chain configurations inside of the lipid bilayer. We now investigate the effects of chain rigidity  $(k_b)$  and tail bead number  $(n_{\rm T})$  of the inclusions on the vesicle fission. For each kind of amphipathic inclusion of fixed  $n_T$  and  $k_b$ , when its concentration is high enough in the simulation box (400 inclusions are applied in all cases), lipid domains will undergo fission from vesicles in most cases. However, under some conditions of  $n_T$  and  $k_b$ , only the configurations of the budding of domains could be observed at the end of the simulations. We summarize the ratio of the occurrence of two configurations of the vesicle with inclusions of different  $n_T$  and  $k_b$  in Figure 7. It is found that the budding configurations of domains occur only when  $n_T$  is larger than 3 and  $k_b \neq 0$ , and the ratio of occurrence of budding increases with the increase of  $n_{\rm T}$  and  $k_{\rm b}$ . The different tail length and chain rigidity of inclusions also influence the evolution of the vesicle fission process. Figure 8 presents the fission durations of the vesicle with the inclusion of different  $n_T$  and  $k_b$  (when  $n_{\rm T}=4$ , we only include the cases in whichthe fission occurs, and the case of  $n_{\rm T}=5$  is excluded because, in most cases of this parameter, fission does not occur). We find that for each  $k_{\rm b}$ , the fission durations are delayed with the increase of  $n_{\rm T}$ . On the other hand, when  $n_T$  is the smallest, changing  $k_b$  has little effect on the fission durations. As  $n_T$  becomes larger, the differences of the fission duration become evident with varying  $k_{\rm b}$ . For a given  $n_{\rm T}$ , the greater that  $k_{\rm b}$  is, the longer the fission duration will be. Furthermore, the effects of the chain structure of inclusions on the vesicle fission are also examined using a vesicle composed of 6400 lipids with a domain size of 6%. The results are consistent with those obtained in the vesicle composed of 3200 lipids.

As with the examples shown in Figure 9a and b, the different tail lengths and chain rigidity will produce different chain configurations of amphipathic inclusions inside of the lipid bilayer. These changes can also be reflected by the mean-square end-to-end distances of the inclusions (Figure 9c). The mean-square end-to-end distance of amphipathic inclusion increases with the increase of  $n_{\rm T}$  and  $k_{\rm b}$ . However, only when  $n_{\rm T}$  and  $k_{\rm b}$  are large enough will their mean-square end-to-end distance be larger than that of lipids located in the outer monolayer. By

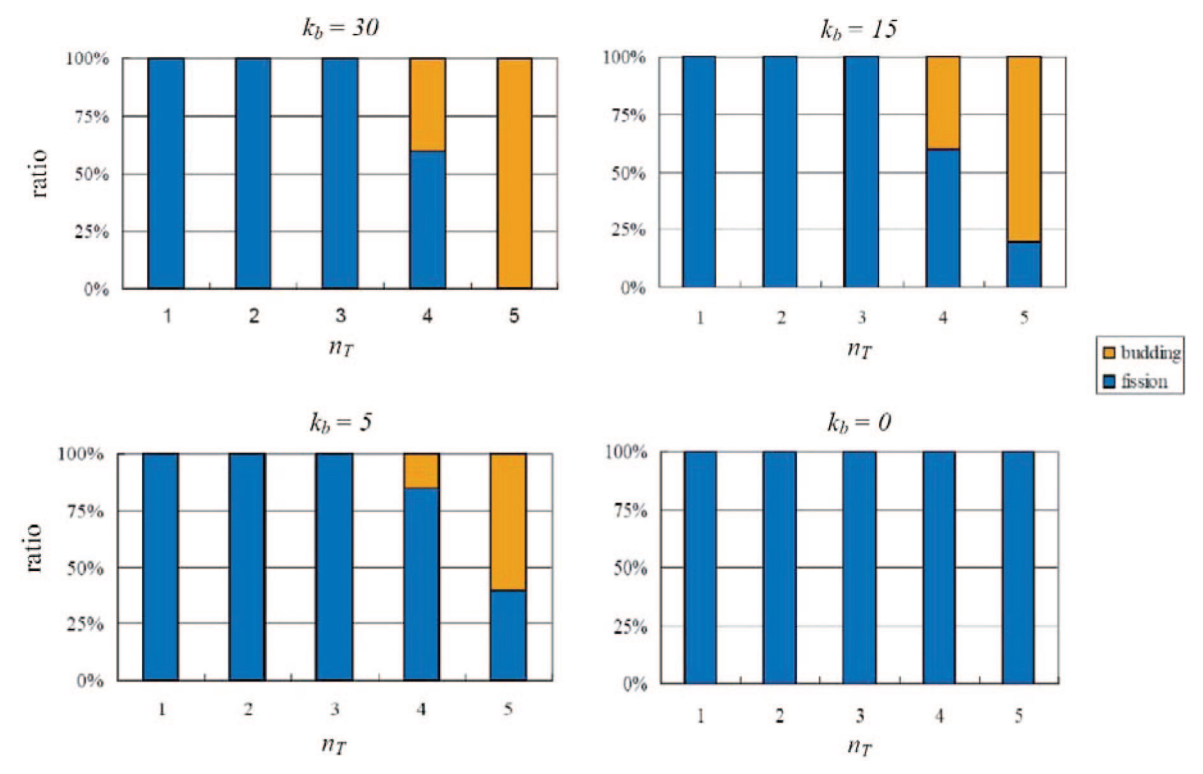


Figure 7. The ratio of the occurrence of budding and fission of the vesicle induced by the inclusion of different tail lengths and chain rigidity. Fission is represented by the blue color, and budding is orange. For each case, at least five independent simulation runs are conducted.

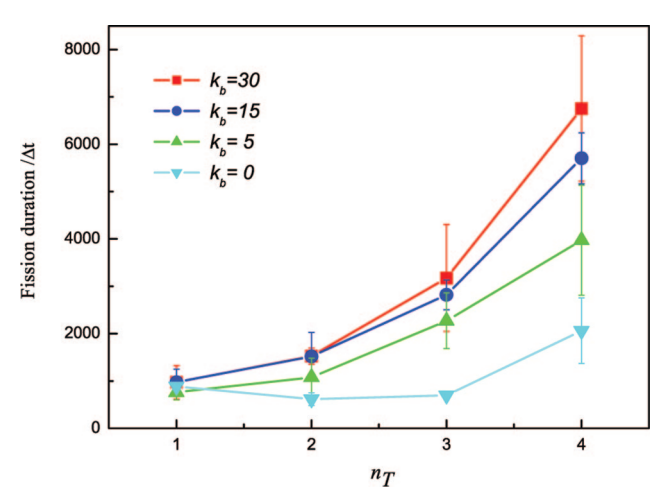


Figure 8. Fission duration with different tail bead numbers and chain rigidity of amphipathic inclusions. The number of amphipathic inclusions is 400, and  $\Pi = 0.81$ .

comparing Figures 7, 8, and 9c, two interesting phenomena are observed. First, the occurrence of budding (Figure 7, orange) exactly corresponds to the cases in Figure 9c in that the inclusions are long or stiff enough (the points in Figure 9c are beyond the dash line). Second, the changes of the fission durations (Figure 8) are very similar to those of the mean-square end-to-end distances of inclusions (Figure 9c). These results suggest that the chain configurations of the inclusions are associated closely with the vesicle fission process, especially when the inclusions are longer and stiffer.

The interaction energy between amphipathic inclusions and the lipid domain could reveal the perturbation of the inclusions on the bilayer and the possible mechanism of shape deformation. The interaction energy is calculated from the bead-bead

conservative interactions between inclusions and B-type lipids

$$E = \begin{cases} \sum \frac{1}{2} a_{ij} \left( 1 - \frac{r_{ij}}{r_{c}} \right)^{2} & r_{ij} < r_{c} \\ 0 & r_{ij} \ge r_{c} \end{cases}$$
 (6)

Here, we choose two groups of inclusions as the example to investigate the interaction of the inclusions of different chain lengths and rigidity with the lipid bilayer and their effects on the vesicle fission. One group is the inclusions of  $k_b = 30$ , but  $n_{\rm T}$  varys from 1 to 5, and the other is the inclusions of  $n_{\rm T}=4$ , but  $k_b$  varys from 0 to 30. Figures 10 and 11 demonstrate the evolution of the interaction energy of the tails of two groups of inclusions with the outer and inner monolayer of the domain, respectively. First, Figures 10 and 11 clearly show that the interaction energy of the inclusions with the outer monolayer is much stronger than that with the inner monolayer. For example, for the inclusion of  $n_T = 1$  and  $k_b = 30$ , its interaction energy with the outer monolayer is about 15 times stronger than that with the inner monolayer. Second, with the variation of  $n_T$ and  $k_{\rm b}$  of inclusions, the interaction energy of the inclusions with two monolayers of the domain is also changed. From Figure 10a, it is found that the energy of the inclusions with the outer monolayer increases with the increase of  $n_T$ . At the same time, the energy of inclusions with the inner monolayer also increases with the increase of  $n_{\rm T}$  (Figure 10b). This demonstrates that the perturbation of the two monolayers by the inclusions increases with the increase of  $n_{\rm T}$ . In addition, when  $n_{\rm T}$  remains unchanged, the configuration of embedded inclusions in the lipid bilayer could also change with the variation of the chain rigidity. This will alter their perturbation on the bilayer. As shown in Figure 11, when  $k_b$  increases, the

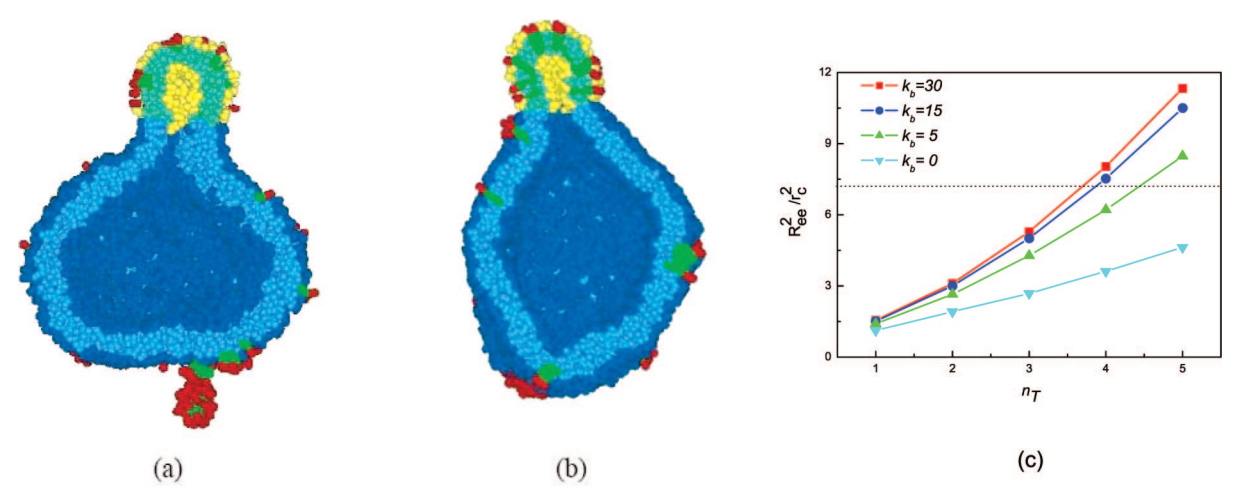


**Figure 9.** The cross-sectional snapshots of the deformation of the vesicle and the domain induced by amphipathic inclusions of (a)  $n_T = 2$ ,  $k_b = 5$  and (b)  $n_T = 5$ ,  $k_b = 30$ . (c) The mean-square end-to-end distances of amphipathic inclusions with different  $n_T$  and  $k_b$ . The dash line in (c) shows the mean-square end-to-end distances of the lipids in the outer monolayer.

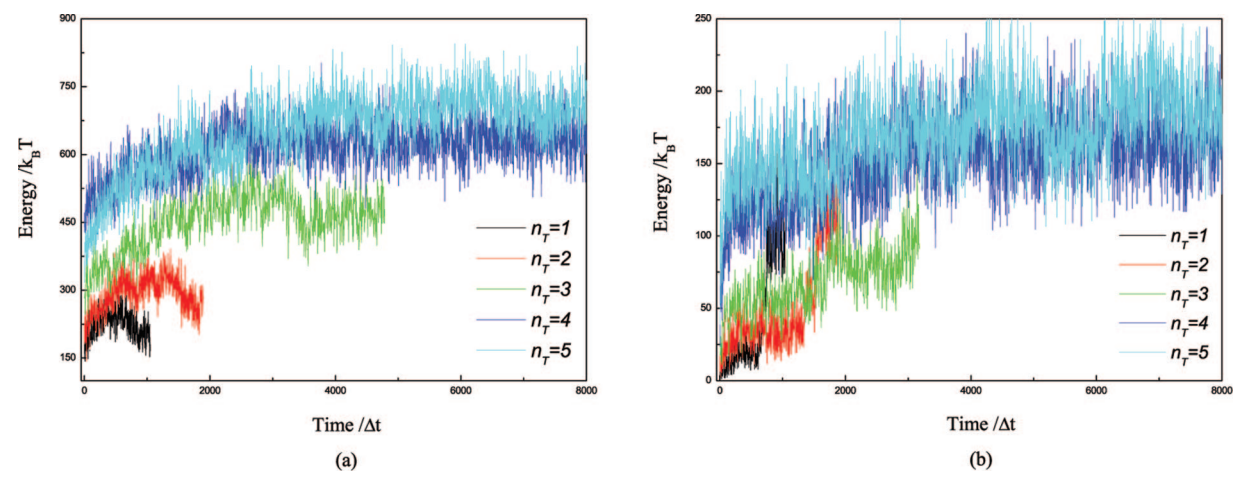


Figure 10. The interaction energy of the tails of the inclusions ( $k_b = 30$  and  $n_T = 1-5$ ) with (a) the outer monolayer and (b) the inner monolayer of the lipid domain. There are 400 amphipathic inclusions.  $\Pi = 0.81$ .

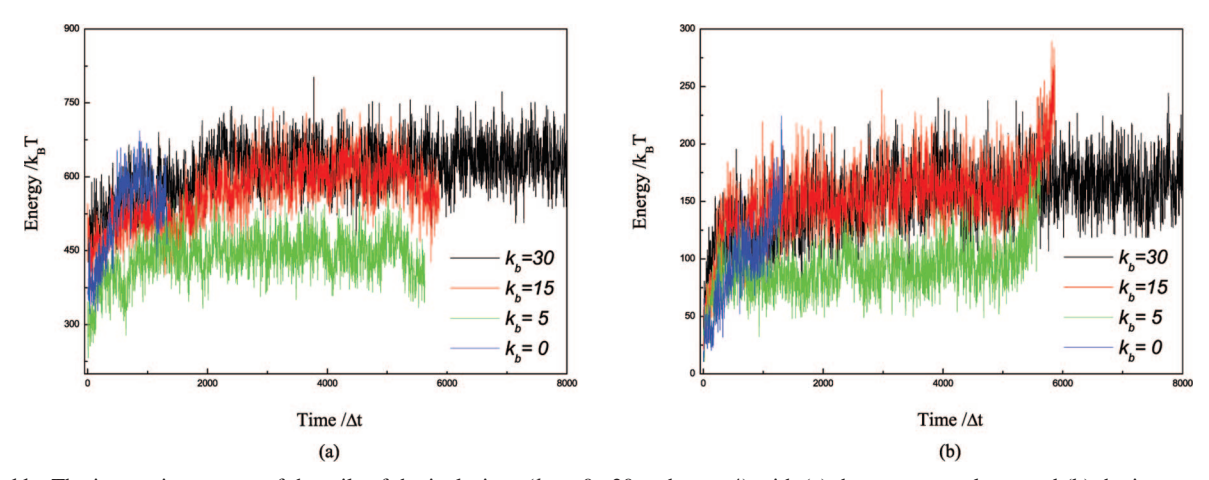


Figure 11. The interaction energy of the tails of the inclusions ( $k_b = 0-30$  and  $n_T = 4$ ) with (a) the outer monolayer and (b) the inner monolayer of the lipid domain. There are 400 amphipathic inclusions.  $\Pi = 0.81$ .

interaction energy of inclusions with both the outer and inner monolayer increases. However, there exists an exceptional case for  $k_b = 0$ , and the change of its energy is relatively rapid and drastic. This may be caused by its almost completely flexible chain. It will be very difficult for the inclusions to stretch inside of the lipid bilayer. Therefore, most inclusion chains could only coil in the outer monolayer and cause the rapid deformation of the outer monolayer. The inner monolayer follows this deforma-

tion, and hence, the interaction between the inclusions and inner monolayer changes rapidly accordingly.

**C.** Effect of the Area-to-Volume Ratio. The effect of the area-to-volume ratio is also important for the shape transformation of a vesicle. It is demonstrated that the shape of a spherical vesicle remains almost unchanged without the change of its interior volume. With the decrease of the interior volume of a vesicle, its area-to-volume ratio increases. Such a change may

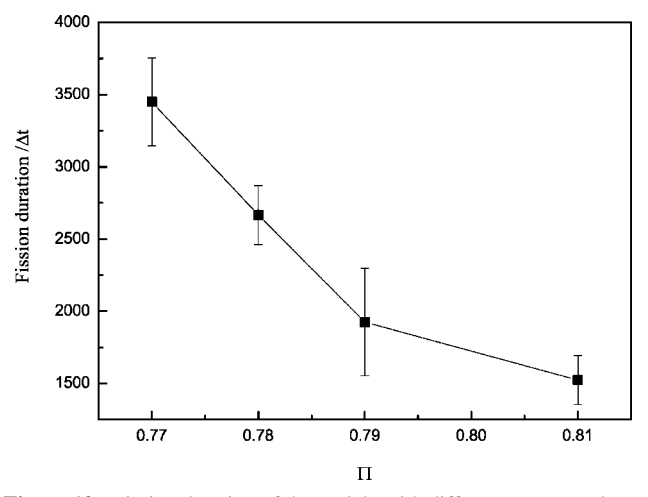


Figure 12. Fission duration of the vesicle with different area-to-volume ratios. The number of amphipathic inclusions is 400, and  $n_T = 2$ .

destroy the mechanical balance between the interior and exterior of the vesicle and promote its shape transformation. It has been experimentally proven that the area-to-volume ratio becomes an effective way to change the shape of a spherical vesicle or

Fission durations with different area-to-volume ratios are shown in Figure 12. We find that with the increase of the areato-volume ratio, the fission process is accelerated. The domain only takes rather short time (about 1500 $\tau$ ) to separate from the parent vesicle. Our simulation results provide a possible way to control the fission processes, especially the fission duration of a vesicle by changing its area-to-volume ratios.

### IV. Discussion

Fission is a highly dynamic process and always requires strong shape deformation of the lipid bilayer. Shape deformation occupies most of the time of the whole fission process and determines the evolution of fission. On the basis of our results, for the vesicles whose sizes we studied, the weak line tension used in our simulations could not solely deform the domain strongly to complete the fission, even when the excess area of the vesicle and domain size further increased or the curvature of parent vesicle decreased. In this case, external amphipathic inclusions play crucial roles. It is indicated that the asymmetric perturbation of amphipathic inclusions on the two monolayers would promote, or even lead to, the shape deformation of the lipid bilayer. Because of its amphipathic structure and initial location, the inclusion inserts itself from the outer monolayer and can not pass through the lipid bilayer completely. As shown in Figure 9c, they are shorter than the lipid molecules, especially when  $n_{\rm T}$  and  $k_{\rm b}$  are small. Therefore, external inclusions are mainly localized in the outer monolayer (Figures 3, 4, and 9). For the lipid bilayer, two monolayers couple together "actively". If one monolayer is perturbed and its lateral organization is changed by the external interaction, the other one will respond to this change spontaneously. In our simulations, the insertion of amphipathic inclusions will compress the lateral packing space of lipids in the outer monolayer, whereas it has little perturbation on the inner monolayer. Such an asymmetric perturbation will break the previous stable state of two monolayers and cause the area difference effect. According to the area difference elasticity theory, the area difference effect can effectively change the shape of the lipid bilayer. 33,34 Under the area difference effect, the bilayer is driven to bulge outwards and gain more space to accommodate both the lipids and inclusions. With the increase of the inclusions in the outer monolayer, the asymmetric perturbation is strengthened. Thus, the area difference effect also becomes stronger accordingly. When the number of amphipathic inclusions is beyond a threshold value, the domain can bud outwards completely under the strong enough area difference effect. Additionally, this asymmetric perturbation can also be reflected by the interaction energy of inclusions with two monolayers. In any case of tail length and chain rigidity of the inclusions, their interaction energy with the outer monolayer is always much stronger than that with the inner monolayer (Figures 10 and 11). The shape deformation of the domain is attributed to such an asymmetric perturbation.

One interesting result of our simulations is that the vesicle fission process will be accelerated or delayed with the variation of the tail length and chain rigidity of the amphipathic inclusions. This phenomenon suggests that the chain configuration of the inclusion inside of the lipid bilayer has an effect on the vesicle fission. When inclusions become longer or stiffer, the deformation of lipid bilayer will be baffled.

It is inferred that the block of the deformation of the lipid bilayer could be caused by two possibilities. One possibility is the decrease of the degree of asymmetric perturbation of the inclusions on the two monolayers. From Figure 9, we can find that with the increase of the tail length and chain rigidity, the inclusions are in a more stretched state, and many tail beads of the inclusions are embedded into the inner monolayer. This will increase the perturbation on the inner monolayer (Figures 10b) and 11b) and reduce the area difference effect between two monolayers. Consequently, the vesicle fission will be delayed, even when the interaction between the inclusions and outer monolayer is strong. The possible effects of the degree of asymmetric perturbation can be sketched in Figure 13. When the sizes of inclusions are short, they are completely localized in the outer monolayer. The insertion of inclusions drives the bulging of the outer monolayer, and the inner monolayer will compensate for this deformation correspondingly (Figure 13a). With the increase of the length of inclusions, the inclusion can reach the inner monolayer. Under the effect of inclusions, the outer monolayer tends to bend outward, as mentioned above. However, the perturbation of the inclusion on the inner monolayer also favors bending of the inner monolayer contrarily. Therefore, the deformation of the bilayer is slightly suppressed, and it needs more time to realize shape deformation (Figure 13b). Once the inclusion is long enough, the deformation degree of two monolayers will be almost identical. Thus, the deformation of two monolayers will counteract each other. In this case, any shape change is hard to obtain (Figure 13c).

The second possibility is the change of the packing state of the inclusions. When a domain buds off from the vesicle, it needs to be strongly bending. Although most inclusions are located in the outer monolayer of the lipid bilayer, their chain configurations are also supposed to change correspondingly (Figure 14). Reasonably, the inclusion will become more difficult to fold with the increase of its tail length and chain rigidity. This may explain why the interaction energy between inclusions and the domain increases with the increase of the tail length and chain rigidity of inclusions (Figures 10 and 11). Thus, for longer or stiffer inclusions, the deformation process will be delayed. Especially in the regions of very high curvature, such as the neck of the bud, all molecules are required to bend fiercely; this possibility will become more important. Furthermore, when the vesicle becomes larger, its curvature decreases. Thus, for the inclusion of the fixed tail length, its perturbation

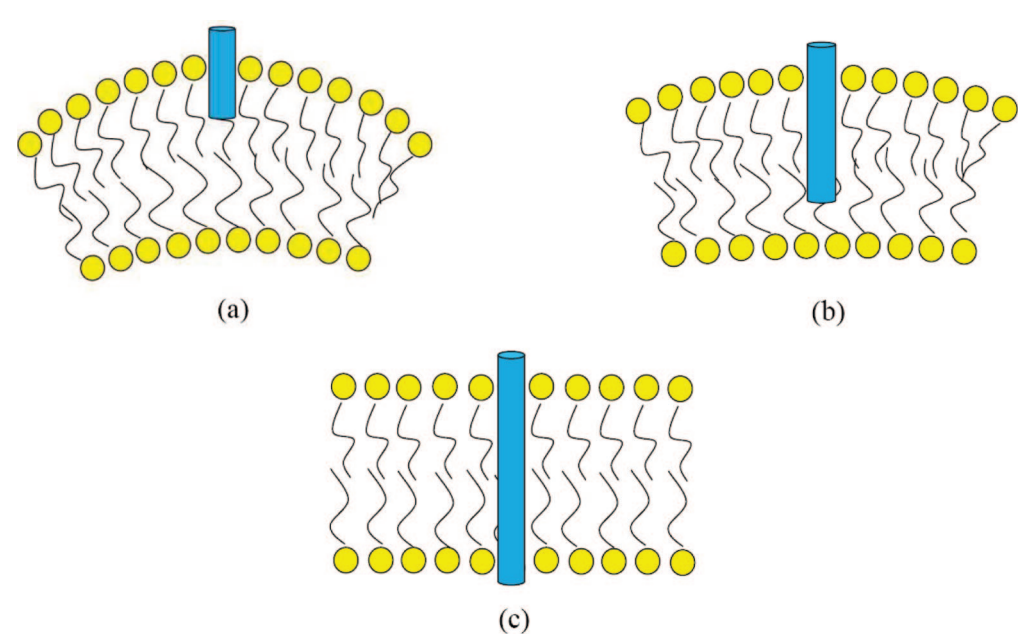
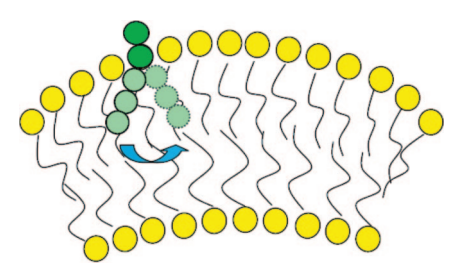


Figure 13. A schematic of the bilayer with embedded inclusions in different lengths.



**Figure 14.** A schematic of the change of the packing state of the inclusions in a deformed lipid bilayer.

on the inner monolayer will also decrease. Therefore, for the large vesicle, the second possibility may become more important.

Conclusively, vesicle fission induced by the external amphipathic inclusions is extremely complicated, and many factors could influence its evolution. The whole fission process can be roughly separated into two stages, shape deformation of the domain and, finally, segregation from the vesicle. It may be mainly attributed to the combined contributions of external inclusions, line tension, area-to-volume ratio, and so forth. They may play roles in the whole process. However, in different stages, the driving factor may be different, especially in the shape deformation stage. Shape deformation is the first step of the fission process. In this stage, it is driven mainly by the insertion of the external inclusions into the domain. The asymmetric distribution of inclusions results in the area difference effect between two monolayers. When their concentration is beyond the threshold value, it will produce enough strong area difference effect to bend the domain outward. However, the deformation of the lipid bilayer is influenced by the structure characters of inclusions simultaneously. With the variety of the chain length and rigidity of inclusions, the degree of shape deformation of the lipid bilayer could be strengthened or weakened. If the domain is strongly deformed and the neck of the bud becomes rather narrow after the first stage, the domain will go on to pinch off from the vesicle. At this time, the majority of the domain has protruded outward, and the shape of bud is near spherical or ellipsoidal. Therefore, the area different effect is possibly weak due to this strong shape deformation of the domain. In the separation stage, the line tension may become important and always intends to minimize the interface length of the domain. Under the effect of line tension of suitable strengthes, the domain can be further curved and rapidly separated from the parent vesicle.

#### V. Conclusion

We studied the behaviors of the budding and fission of a twocomponent lipid vesicle induced by the external amphipathic inclusions using the DPD method. We found that vesicle fission is collectively regulated by the area-to-volume ratio of the vesicle, the inclusions' concentration, the molecular structure of amphipathic inclusions, and so forth. Our results indicate that vesicle fission results from a combination of the domain's line tension and a threshold number of amphipathic inclusions. Especially, the chain length and rigidity of amphipathic inclusions can affect both the probability of fission and its duration. Additionally, increasing the vesicle's area-to-volume ratio for a vesicle/inclusion system that would successfully undergo fission reduces the time required for the fission to occur. The present work also provides a possible model for the controlleddrug-releasing system. Actually, the lipid vesicle is one of the most widely studied drug carriers.<sup>36</sup> Our simulations indicate that the fission behavior of a vesicle can be controlled by adjusting the concentration and the molecular structure of amphipathic inclusions or the area-to-volume ratio of the lipid vesicle.

**Acknowledgment.** This work was supported by the National Basic Research Program of China, No. 2007CB925101, and the National Natural Science Foundation of China, Nos. 10574061, 10629401, and 20674037.

### **References and Notes**

- (1) Mouritsen, O. G. *Life—as a matter of fat*; Springer-Verlag: Berlin, Germany, 2005.
  - (2) Simons, K.; Toomre, D. Nat. Rev. Mol. Cell Biol. 2001, 1, 31.
  - (3) Shaw, A. S. Nat Immunol. 2006, 7, 1139.
  - (4) Feigenson, G. W. Nat. Chem. Biol. 2006, 2, 560.
  - (5) Veatch, S. L.; Keller, S. L. Phys. Rev. Lett. 2002, 89, 268101.
  - (6) McMahon, H. T.; Gallop, J. L. Nature 2005, 438, 590.
- (7) Bacia, K.; Schwille, P.; Kurzchalia, T. Proc. Natl. Acad. Sci. U.S.A. 2005, 102, 3272.

- (8) Hamada, T.; Miura, Y.; Ishii, K.; Araki, S.; Yoshikawa, K.; Vestergaard, M.; Takagi, M. J. Phys. Chem. B 2007, 111, 10853.
- (9) Ford, M. J.; Miller, I. G.; Peter, B. J.; Vallis, Y.; Gerrit, J. K.; Praefcke, G.J. K.; Evans, P. R.; McMahon, H. T. Nature 2002, 419, 361.
- (10) Peter, B. J.; Kent, H. M.; Mills, I. G.; Vallis, Y.; Butler, P. J. G.; Evans, P. R.; McMahon, H. T. Science 2004, 303, 495
  - (11) Lee, M. C. S.; Schekman, R. Science 2004, 303, 479.
  - (12) Habermann, B. EMBO Rep. 2004, 5, 250.
- (13) Masuda, M.; Takeda, S.; Sone, M.; Ohki, T.; Mori, H.; Kamioka, Y.; Mochizuki, N. EMBO J. 2006, 25, 2889.
  - (14) Inaoka, Y.; Yamazaki, M. Langmuir 2007, 23, 720.
- (15) Tanaka, T.; Sano, R.; Yamashita, Y.; Yamazaki, M. Langmuir 2004, 20, 9526.
- (16) Zimmerberg, J.; Kozlov, M. M. Nat. Rev. Mol. Cell Biol. 2006, 7,
  - (17) Jülicher, F.; Lipowsky, R. Phys. Rev. Lett. 1993, 70, 2964.
  - (18) Maruvka, Y. E.; Shnerb, N. M. Phys. Rev. E 2006, 73, 011903.
  - (19) Hyvönen, M. T.; Kovanen, P. T. Eur. Biophys. J. 2005, 34, 294.
- (20) Shinoda, W.; Namiki, N.; Okazaki, S. J. Chem. Phys. 1997, 106, 5731.
- (21) Reynwar, B. J.; Illya1, G.; Harmandaris1, V. A.; Muller, M. M.; Kremer, K.; Deserno, M. Nature 2007, 447, 461.
- (22) Markvoort, A. J.; Smeijers, A. F.; Pieterse, K.; van Santen, R. A.; Hilbers, P. A. J. J. Phys. Chem. B 2007, 111, 5719.

- (23) Cooke, I. R.; Kremer, K.; Deserno, M. Phys. Rev. E 2005, 72, 011506.
  - (24) Shillcock, J. C.; Lipowsky, R. J. Chem. Phys. 2002, 117, 5048.
- (25) Grafmuller, A.; Shillcock, J. C.; Lipowsky, R. Phys. Rev. Lett. 2007, 98, 218101.
  - (26) Laradji, M.; Kumar, P. B. S. Phys. Rev. Lett. 2004, 93, 198105.
  - (27) Yamamotoa, S.; Hyodo, S. J. Chem. Phys. 2003, 118, 7937.
- (28) Li, D. W.; Liu, X. Y.; Feng, Y. P. J. Phys. Chem. B 2004, 108, 11206
- (29) Hoogerbrugge, P. J.; Koelman, J. M. V. A. Europhys. Lett. 1992, 19, 155.
  - (30) Espagnol, P.; Warren, P. Europhys. Lett. 1995, 30, 191.
- (31) Vattulainen, I.; Karttunen, M.; Besold, G.; Polson, J. M. J. Chem. Phys. 2002, 116, 3967.
- (32) Yanagisawa, M.; Imai, M.; Taniguchi, T. Phys. Rev. Lett. 2008, 100, 148102.
  - (33) Seifert, U. Adv. Phys. 1997, 46, 13.
- (34) Miao, L.; Seifert, U.; Wortis, M.; Dobereiner, H. Phys. Rev. E 1994, 49, 5389.
- (35) Jakobsen, A. F.; Mouritsen, O. G.; Besold, G. J. Chem. Phys. 2005, 122, 204901.
- (36) Yang, L.; Alexandridis, P. Curr. Opin. Colloid Interface Sci. 2000, 5, 132.

JP805551S